JOURNAL OF GENERAL VIROLOGY

RESEARCH ARTICLE

Falci Finardi *et al.*, *Journal of General Virology* 2021;102:001702

DOI 10.1099/jgv.0.001702

MICROBIOLOGY SOCIETY

OPEN ACCESS

Identification and characterization of bisbenzimide compounds that inhibit human cytomegalovirus replication

Nicole Falci Finardi[1]†, HyeongJun Kim[2,3], Lee Z. Hernandez[2,3,4], Matthew R. G. Russell[5], Catherine M-K Ho[1], Vattipally B. Sreenu[6], Hannah A. Wenham[1], Andy Merritt[7] and Blair L. Strang[1,8,*,†]

Abstract

The shortcomings of current anti-human cytomegalovirus (HCMV) drugs has stimulated a search for anti-HCMV compounds with novel targets. We screened collections of bioactive compounds and identified a range of compounds with the potential to inhibit HCMV replication. Of these compounds, we selected bisbenzimide compound RO-90-7501 for further study. We generated analogues of RO-90-7501 and found that one compound, MRT00210423, had increased anti-HCMV activity compared to RO-90-7501. Using a combination of compound analogues, microscopy and biochemical assays we found RO-90-7501 and MRT00210423 interacted with DNA. In single molecule microscopy experiments we found RO-90-7501, but not MRT00210423, was able to compact DNA, suggesting that compaction of DNA was non-obligatory for anti-HCMV effects. Using bioinformatics analysis, we found that there were many putative bisbenzimide binding sites in the HCMV DNA genome. However, using western blotting, quantitative PCR and electron microscopy, we found that at a concentration able to inhibit HCMV replication our compounds had little or no effect on production of certain HCMV proteins or DNA synthesis, but did have a notable inhibitory effect on HCMV capsid production. We reasoned that these effects may have involved binding of our compounds to the HCMV genome and/or host cell chromatin. Therefore, our data expand our understanding of compounds with anti-HCMV activity and suggest targeting of DNA with bisbenzimide compounds may be a useful anti-HCMV strategy.

INTRODUCTION

Disease caused by human cytomegalovirus (HCMV) is wide ranging and has significant social and economic impact [1]. Currently, there is no widely available vaccine against HCMV [1, 2]. Plus, the use of first- and second-line antiviral drugs inhibiting the HCMV DNA polymerase (ganciclovir and foscarnet) have a number of shortcomings, including the development of antiviral resistance [3].

The identification of novel anti-HCMV drugs [4, 5] has focused on finding compounds that inhibit the function of a limited number of HCMV proteins, including the HCMV kinase UL97 and the HCMV DNA packaging complex proteins [5, 6]. However, like ganciclovir and foscarnet, novel anti-HCMV drugs targeting UL97, or DNA packaging complex proteins, also have significant issues with the development of antiviral resistance [7–12] or are thought to have poor efficacy in clinical trials [13, 14]. To overcome the development of antiviral resistance when targeting proteins expressed by HCMV, there has been interest in inhibiting the function of cellular proteins required for HCMV replication. The stability of the cellular genome would limit the occurrence of mutations that would allow anti-viral resistance to occur.

A number of cellular proteins required for HCMV replication have been identified [15] and there have been efforts to identify compounds known to inhibit the function of cellular proteins required for anti-HCMV replication (some examples

Received 23 August 2021; Accepted 20 October 2021; Published 09 December 2021

Author affiliations: [1]Institute of Infection & Immunity, St George's, University of London, London, UK; [2]Department of Physics and Astronomy, University of Texas Rio Grande Valley, Edinburg, TX, USA; [3]Biochemistry and Molecular Biology Program, University of Texas Rio Grande Valley, Edinburg, TX, USA; [4]Department of Physics, Applied Physics and Astronomy, Rensselaer Polytechnic Institute, Troy, NY, USA; [5]The Francis Crick Institute, London, UK; [6]MRC – University of Glasgow Centre for Virus Research, University of Glasgow, Glasgow, UK; [7]Centre for Therapeutic Discovery, LifeArc, Stevenage, UK; [8]Department of Biological Chemistry & Molecular Pharmacology, Harvard Medical School, Boston, MA, USA.

***Correspondence:** Blair L. Strang, bstrang@sgul.ac.uk

Keywords: bisbenzimide; drug ; human cytomegalovirus.

Abbreviations: HCMV, human cytomegalovirus; HFF, human foreskin fibroblast; IFN, Interferon; LOPAC, Library of Pharmacologically Active Compounds; NIH, National Institutes of Health.

†These authors contributed equally to this work

Eight supplementary tables and three supplementary figures are available with the online version of this article.

of which can be found in the literature [16–22]). However, none of the compounds identified in the aforementioned works have progressed toward clinical development due to a number of factors, for example polypharmacology of the compounds identified.

Novel strategies for inhibition of HCMV replication need to be explored. To this end, we decided to screen compounds with known bioactive activity for anti-HCMV activity.

METHODS

Cells and viruses

Human foreskin fibroblast (HFF) cells (clone Hs29) were obtained from American Type Culture Collection no. CRL-1684 (ATCC). All cells were maintained in complete media: Dulbecco's modified Eagle medium (DMEM) containing 10% FBS, plus penicillin and streptomycin (all Gibco). HCMV strains AD169 and Merlin(R1111) were kindly provided by Don Coen (Harvard Medical School) and Richard Stanton (Cardiff University), respectively.

Compound collections

The Microsource-1 US Drug Collection (Discover Systems) contained compounds that had reached clinical trial stage in the USA. LOPAC 1 (Sigma-Aldrich) contained known pharmacologically active compounds. NIH Clinical Collection (BioFocus) comprised the 2012 versions of compound collections NCC1 and NCC2, which contained compounds that had a history of use in clinical trials. All compounds were resuspended in DMSO (stock solution concentrations for each collection were 2 mg ml^{-1}, 10 mM and 10 mM, respectively).

High-throughput screening of compounds

We have previously described infection of HFF cells with HCMV strain AD169 for high-throughput screening, preparation of screening plates for high-throughput microscopy analysis, microscopy analysis of screening plates and analysis of screening results in several works describing screening small molecules and small interfering RNA (siRNA) collections [20–23]. The experimental methodology is described in the results section. The final amount of each compound in the screening assay was: Microsource – 200 ng, LOPAC – 28 µM, NIH – 28 µM.

To assess the quality of data that could be returned from the screening protocol, we calculated the Z'-factor [24, 25] derived from the positive (heparan sulphate-treated infected cells) and negative (DMSO-treated infected cells) control wells. The screening controls for one plate in the LOPAC collection returned Z'-factors of <0.5. Thus, the data from that plate were discarded. All other screening plates returned Z'-factors ≥0.5, indicating a robust separation of difference in the data derived from positive and negative controls.

Compounds

RO-90-7501 (2′-(4-aminophenyl)-[2,5′-bi-1*H*-benzimidazol]−5-amine) was purchased from Tocris. We synthesized MRT00210423, MRT00210424, MRT00210425, MRT00210426 and MRT00210427 using the schemes shown in Fig. S1 (available in the online version of this article). All compounds were resuspended in DMSO.

Viral yield reduction assays

Assays were performed essentially as described previously [26]. HFF cells were plated at 5×10^4 cells per well in 24-well plates. After overnight incubation, cells were infected with HCMV at an m.o.i. of 1. After virus adsorption for 1 h at 37 °C, cells were washed and incubated with 0.5 ml of media containing DMSO or compounds at a range of concentrations. Plates were incubated for 4 days at 37 °C. Titres were determined by serial dilution of viral supernatant onto HFF monolayers which were covered in DMEM containing 5% FBS, 0.6% methylcellulose and antibiotics. Cultures were incubated for 14 days, cells were stained with crystal violet and plaques were counted. The final concentration of DMSO in all samples was maintained at <1% (v/v). The EC_{50} value of data from this assay was calculated using GraphPad.

MTT cytotoxicity assays

Assays were performed essentially as described [26]. In this colorimetric assay the ability of cellular NAD(P)H-dependent cellular oxidoreductase enzymes to reduce the tetrazolium dye 3-(4,5-dimethylthiazol-2-yl)−2,5-diphenyltetrazolium bromide (MTT) to formazan was measured. HFF cells were seeded at 1×10^4 or 1×10^3 cells per well into 96-well plates. High concentrations of cells (1×10^4 per well) should allow assessment of cell viability, whereas low concentrations of cells (1×10^3 per well) should allow assessment of both cell viability and cell proliferation. After overnight incubation to allow cell attachment, cells were treated for 96 h with a range of concentrations of compound, or the equivalent volume of DMSO. MTT assays were then performed according to the manufacturer's instructions (GE Healthcare). The final concentration of DMSO in all samples was maintained at <1% (v/v).

Light microscopy

HFF cells were seeded in 24-well tissue culture plates (5×10^4 cells per well). Twenty-four hours later, cells were treated with the concentrations of compound indicated in the text or the equivalent volume of DMSO in complete media. After 1 h of incubation with compounds or DMSO at 37 °C, cells were placed at room temperature followed by incubation with ice cold methanol (30 min). Cells were washed with PBS and imaged using a Zeiss Axioplan 2 microscope.

Agarose gel electrophoresis

Plasmid pUC19 (a kind gift from Steve Goodbourn, St George's, University of London) was linearized by digestion with enzyme *Eco*RI using the supplier's (New England Biolabs) instructions. A 0.8% TAE agarose gel was prepared with compound added to a concentration of 10 µM and the linearized plasmid was introduced into the gel via electrophoresis. Also introduced into the gel was a ladder of

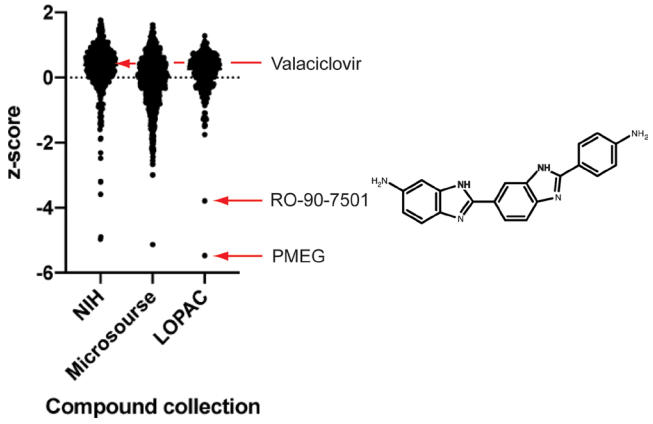

Fig. 1. Compounds assigned z-scores. The ability of compounds within the NIH Clinical, Microsource and LOPAC collections to inhibit HCMV strain AD169 pp28 protein production in HFF cells was investigated. After exclusion of compounds judged to be cytotoxic, each compound was assigned a z-score (the number of standard deviations from the mean value of the screen) to describe the number of cells expressing the HCMV antigen pp28. Thus, negative and positive z-scores represented fewer or greater numbers of cells expressing pp28, respectively. A plot of all z-scores is shown for each collection, where each data point represents a single compound. Lists of compounds from each collection with their assigned z-scores are shown in Tables S4-S6. The z-scores of RO-90-7501, PMEG and valaciclovir are indicated with red arrows. The structure of RO-90-7501 is also shown.

DNA markers (N3232S; New England Biolabs). The gel was exposed to UV light and images of the gel were captured using a Syngene camera apparatus.

Analysis of putative binding sites in the HCMV genome

The complete analysis pipeline along with the source code is available on the GitHub page (https://github.com/vbsreenu/find-motif). Briefly, genome sequences in fasta format and gene features in gff format were downloaded from GenBank with the help of NCBI's eutils API (scripts are available on GitHub: https://github.com/vbsreenu/find-motif). Using a custom FIND_MOTIF program, nucleotide motifs were extracted from genome sequence files and their corresponding gene features from the gff file. The FIND_MOTIF program was developed in C programming language using a Karp-Robin string search algorithm to find nucleotide motifs (kmers) in the genome sequence file. The locations of the motifs were then compared with a genome features table file using an AWK script to find whether the motifs were part of any coding region. Final results were stored in a specified output file.

Dual labeling of bacteriophage lambda genomic DNA for single-molecule microscopy

Bacteriophage lambda genomic DNA (lambda DNA) with a digoxigenin moiety at one terminus (to label DNA with a quantum dot) and a biotin moiety at the other terminus (to tether the DNA onto the surface of a microfluidic flow cell through biotin–neutravidin interaction) was prepared as previously described elsewhere [27]. Briefly, lambda DNA had 12 nt overhangs at both ends. Biotin-labelled (5′-aggtcgccgccc/3′BioTEG/-3′) and digoxigenin (5′-gggcggcgacctaaaaaaaaaaaa/3′Dig_N)-labelled oligos complementary to the overhangs were annealed and ligated to lambda DNA. The ligation reaction mixture was run on a 0.4% agarose gel, allowing unconjugated excess oligos to be separated from labelled DNA by electrophoresis. The DNA band corresponding to the biotin- and digoxigenin-labelled lambda DNA was excised from the gel. The purified biotin- and digoxigenin-labelled lambda DNA was recovered from the excised agarose gel in a dialysis bag and concentrated using an ethanol precipitation of DNA procedure.

Preparation of a flow cell for single-molecule microscopy flow-stretching assays

A microfluidic flow cell was assembled using a quartz top, a surface-passivated cover glass (using polyethylene glycol), double-sided tape, and inlet and outlet tubes as previously described elsewhere [27, 28]. Approximately 4% of the polyethylene glycol layer on the cover glass had biotin moieties onto which were tethered the dual labelled lambda DNAs described above. To fix the dual labelled lambda DNA to the glass cover, 0.25 mg ml^{-1} neutravidin was added to the flow cell and incubated for at least 5 min. The excess neutravidin was removed by flowing Qdot-labelling buffer (10 mM Tris, pH 8.0, 150 mM NaCl, 10 mM $MgCl_2$, 0.2 mg ml^{-1} BSA) into the flow cell. Then, the biotin- and digoxigenin-labelled lambda DNA was flowed into the flow cell at a rate of 30 µl min^{-1}. Excess dual labelled DNAs not joined to the cover glass surface were removed by flowing in Qdot-labelling buffer. Quantum dots were affixed to DNA by flowing 250 µl of 750-fold diluted anti-digoxigenin-conjugated quantum dot 605 (Thermo Fisher Scientific S10469, anti-digoxigenin antibody: GeneTex GTX73152) at a rate of 30 µl min^{-1}. The flow cell was washed to remove the excess quantum dots by flowing imaging buffer (20 mM Tris, pH 7.5, 150 mM NaCl, 2 mM $MgCl_2$, 1.2 mg ml^{-1} BSA) into the flow cell at a rate of 50 µl min^{-1}.

Data capture and analysis in single-molecule DNA flow-stretching assays

Each compound was diluted in imaging buffer containing BSA at the concentrations mentioned in the text. Compound or DMSO were flowed into the cell at a rate of 50 µl min^{-1}. Quantum dots labelled on lambda DNA were imaged under a total internal reflection fluorescence microscope with 532 nm laser illumination. Movement of quantum dots (Lamdba DNA compaction events) were recorded using Micro-Manager software [29] and, subsequently, kymographs were prepared using ImageJ [30].

Western blotting

HFF cells (5×10^4 cells per well) were infected with virus (m.o.i. 1) and treated with the concentrations of compounds indicated in the text or the equivalent volume of DMSO.

Table 1. Compounds assigned low z-scores in the screening assay

Compound	ChEMBL ID	Library	z-score
AM-251	CHEMBL285932	NIH Clinical Collection	−2.1
Ancitabine HCl	CHEMBL1412614	LOPAC	−3.0
Aurintricarboxylic acid	CHEMBL275938	LOPAC	−3.6
S-(*p*-Azidophenacyl) glutathione	–	LOPAC	−2.1
Carboplatin	CHEMBL1351	Microscource	−5.1
Cetirizine HCl	CHEMBL1000	Microscource	−2.1
Chloroxylenol	CHEMBL398440	Microscource	−2.1
Clonazepam	CHEMBL452	Microscource	−2.2
Clopidol	CHEMBL446918	Microscource	−2.1
Dibenzothiophene	CHEMBL219828	Microscource	−2.0
Floxuridine	CHEMBL917	NIH Clinical Collection	−3.5
Fludarabine	CHEMBL1568	NIH Clinical Collection	−3.2
Hexachlorophene	CHEMBL496	NIH Clinical Collection	−4.9
Hexylresorcinol	CHEMBL443605	Microscource	−2.0
Lisinopril	CHEMBL1237	Microscource	−2.1
Methotrexate	CHEMBL426	Microscource	−2.9
PMEG	CHEMBL20283	LOPAC	−5.4
Pyrimethamine	CHEMBL36	Microscource	−2.1
Raltitrexed	CHEMBL225071	NIH Clinical Collection	−3.0
Ranolazine	CHEMBL1404	Microscource	−2.2
Rifaximin	CHEMBL1617	Microscource	−2.3
RO-90-7501	–	LOPAC	−3.8
Salicylanilide	CHEMBL82970	Microscource	−2.0
Tamoxifen	CHEMBL83	Microscource	−2.5
Tenoxicam	CHEMBL302795	Microscource	−2.6
Unknown	–	NIH Clinical Collection	−2.4
Xylometazoline HCl	CHEMBL312448	Microscource	−2.1

z-score (-2.0)-(-2.9) (-3.0)-(-3.9) (-4.0)-(-4.9) (-5.0)-(-5.9)

All samples were prepared for western blotting by washing cells once in PBS, then suspending cells directly in 50 µl 2× Laemmli buffer containing 5% β-mercaptoethanol before incubating at 95 °C for 5 min. Western blotting of proteins was carried out as described elsewhere [31], using antibodies recognizing IE1/2, UL57, pp28, (all Virusys, 1:1000 dilution), UL86 (a kind gift from Wade Gibson, Johns Hopkins School of Medicine, 1:1000 dilution) and β-actin (Sigma, 1:5000 dilution). All primary antibodies were incubated overnight at 4 °C and detected using an anti-mouse- or anti-rabbit-HRP-conjugated antibody (New England Biolabs). Chemiluminescence solution (GE Healthcare) was used to detect secondary antibodies on film.

Real time quantitative PCR analysis of viral DNA synthesis in HCMV-infected cells

Preparation of samples for PCR and PCR analysis were conducted using the methodology and reagents we have described elsewhere [23, 32, 33] to calculate the number of copies of the viral gene *UL83* per copy of the cellular gene *adipsin*. Statistical analysis was performed using Graphpad.

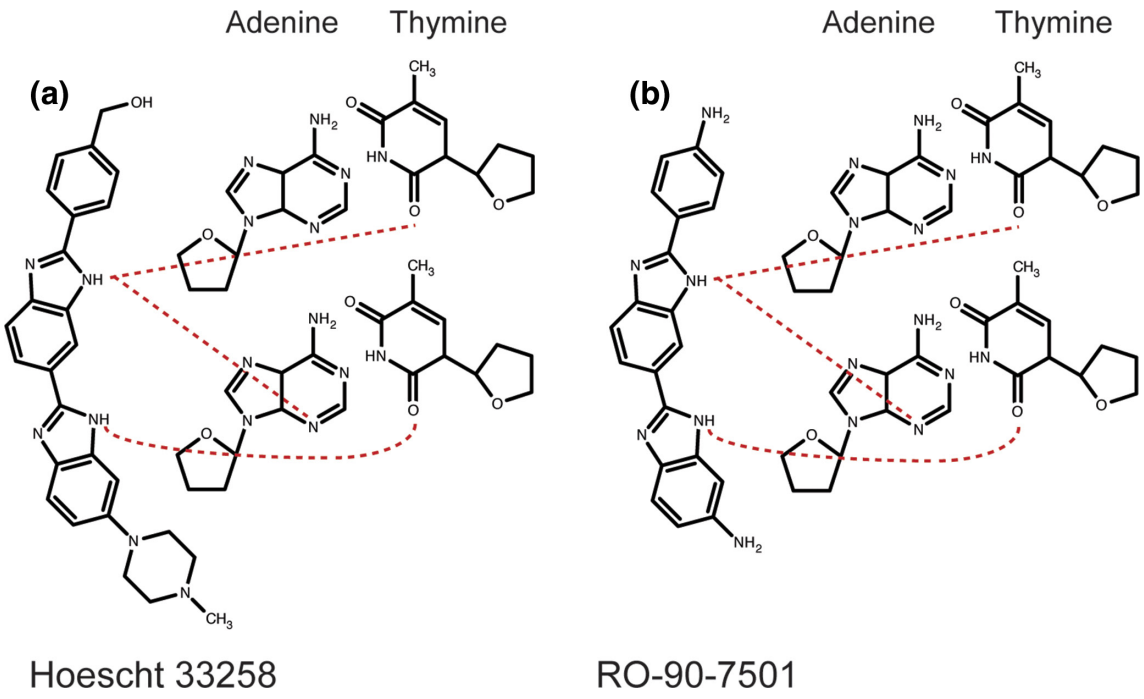

Fig. 2. Structure of bisbenzimide compounds. (a) The structure of Hoechst 33258. The binding of Hoechst 33258 to DNA via hydrogen bonds between amine groups in Hoechst 33258 and oxygen and nitrogen atoms in adenine and thymine nucleotides [40] is indicated with red dotted lines. (b) The structure of RO-90-7501; the predicted binding of this compound to DNA via hydrogen bonding is indicated by red dotted lines.

Electron microscopy analysis of HCMV-infected cells

HCMV-infected HFF cells were treated as outlined in the figure legends. To prepare cells for analysis, cells were incubated for 1 h at room temperature in fixative (1.5% glutaraldehyde and 4% paraformaldehyde in 0.1 M sodium cacodylate buffer, pH 7.4). After fixation, cells were washed three times for 15 min in 0.1 M sodium phosphate buffer (pH 7.4) and dehydrated in ethanol (50, 70, 90%, 15 min wash each). Cells were then washed in 90% ethanol containing LR-White embedding medium (2 h) and transferred to gelatin capsules (polymerization at 55 °C for 24 h).

Eighty-nanometre sections of each capsule were stained with lead citrate and imaged in a 1400 FLASH transmission electron microscope (JEOL) at −2 µm defocus with 2.8 nm pixels using 2×2 TEM centre montaging. Montages were then converted to mrc format and contrast adjusted, before outputting as a 1:1 tif series with the 'movie' function, using the tif2mrc and 3dmod packages of IMOD [34].

RESULTS

Screening of bioactive compound collections

We have previously employed an automated high-throughput screening methodology to identify compounds and siRNAs with potential anti-HCMV activity [20–23]. We used this methodology to screen collections of bioactive compounds in the NIH Clinical, Microsource and LOPAC collections for potential anti-HCMV activity. Briefly, cells infected with the high-passage HCMV strain AD169 [35] were treated with compounds from each collection. Two factors were then assayed using automated microscopy: the number of cells in each well and the number of cells expressing the HCMV antigen pp28. pp28 is essential for HCMV replication [36] and its expression late in HCMV replication is dependent on viral DNA synthesis [37]. Therefore, our screen had the potential to identify compounds able to inhibit several stages of HCMV replication, including viral DNA synthesis. Those compounds that produced a decrease in the number of cells in the assay by 50% or greater were judged to be cytotoxic to HCMV-infected cells (Tables S1–S3) and were not studied further. The remaining data from the screen were then converted to a z-score (the number of standard deviations from the mean of the data [24, 25]) to show an increase or decrease in the number of cells expressing pp28 (positive or negative z-score, respectively) (Fig. 1, Tables S4–S6).

We investigated if our screening results were consistent with the activity of known antiviral compounds and data previously reported using these compound collections. We noted that one antiviral compound with known anti-HCMV activity, PMEG [38], was assigned a negative z-score (−5.4; Fig. 1, Table S6), while an antiviral compound known to have poor anti-HCMV activity, valaciclovir [39], was assigned a z-score close to zero (0.4; Fig. 1, Table S4). Therefore, our

screening data were consistent with the known anti-HCMV activity of at least two compounds.

To our knowledge, the NIH Clinical Collection used here has not been previously used to identify compounds with anti-HCMV activity. The Microsource collection has been used in screening experiments to identify compounds with anti-HCMV activity [16–18]. However, these screens had different parameters to our own (inhibition of ectopic GFP expression controlled by viral protein IE2 [16], inhibition of IE2-YFP fusion protein expression from a recombinant HCMV virus [17] and inhibition of fusion protein pp28-GFP expression from a recombinant HCMV virus [18]) and, therefore, reported considerably different results. Screening of the LOPAC collection for anti-HCMV activity using an assay different to our own has been reported [19], but the screening methodology and the full list of compounds with anti-HCMV activity found in the aforementioned screen have not been reported [19]. Therefore, it was not possible to compare our data with the previously reported screen of the LOPAC collection.

We also considered whether some compounds were routinely identified in a range of screens due to an unappreciated non-specific effect of the compound. All three compound collections examined here have been used in a range of screens, some mentioned above. To our knowledge, no other screening experiment has reported the same findings as our screens. Therefore, the compounds we identified in our screen may have had a specific anti-HCMV activity and were unlikely to be identified due an unappreciated non-specific activity of the compound.

The compounds assigned low z-scores (less than −2.0) in each collection were examined further (Table 1). A wide range of compounds were found to inhibit the expression of pp28 in our assay. Expression of pp28 is dependent on viral DNA synthesis [37], which was consistent with compounds known to inhibit viral DNA synthesis (PMEG) being assigned the lowest z-scores (Table 1). However, it was unclear or unknown how a number of other compounds assigned low z-scores (including aurintricarboxylic acid, floxuridine, fludarabine or hexachlorophene; Table 1) affected pp28 expression.

We then decided to choose a compound in Table 1 for further investigation. We sought a compound that had a low z-score, had not previously been reported to inhibit HCMV, may have had a target other than a viral or cellular protein, and could be amenable to modification. Based on these criteria, we chose to investigate how RO-90-7501 (Fig. 1) might inhibit HCMV replication.

To our knowledge, there were no previous reports that RO-90-7501 could inhibit HCMV replication. RO-90-7501 is

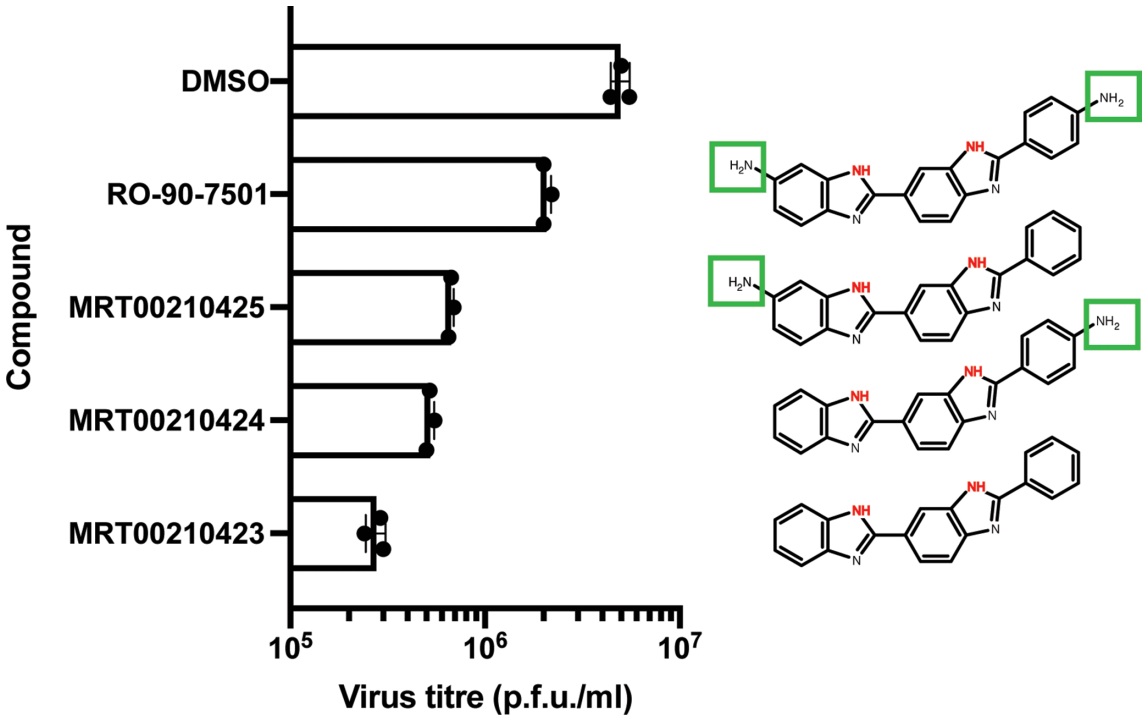

Fig. 3. Anti-HCMV activity of RO-90-7501 analogues. HFF cells were infected with HCMV strain AD169 (m.o.i. 1) in the presence of the compounds indicated in the figure (1 µM) or the equivalent volume of DMSO. At 96 h post-infection, virus titre (p.f.u. ml^{-1}) from these infections was determined. The data points from three independent experiments are shown. The columns and error bars represent the mean and SD, respectively, of those data points. The structures of the bisbenzimide compounds examined are shown to the right of the figure. Amine groups thought to be involved in DNA binding in each compound are highlighted in red text. Terminal amine groups of the compounds are highlighted in green boxes.

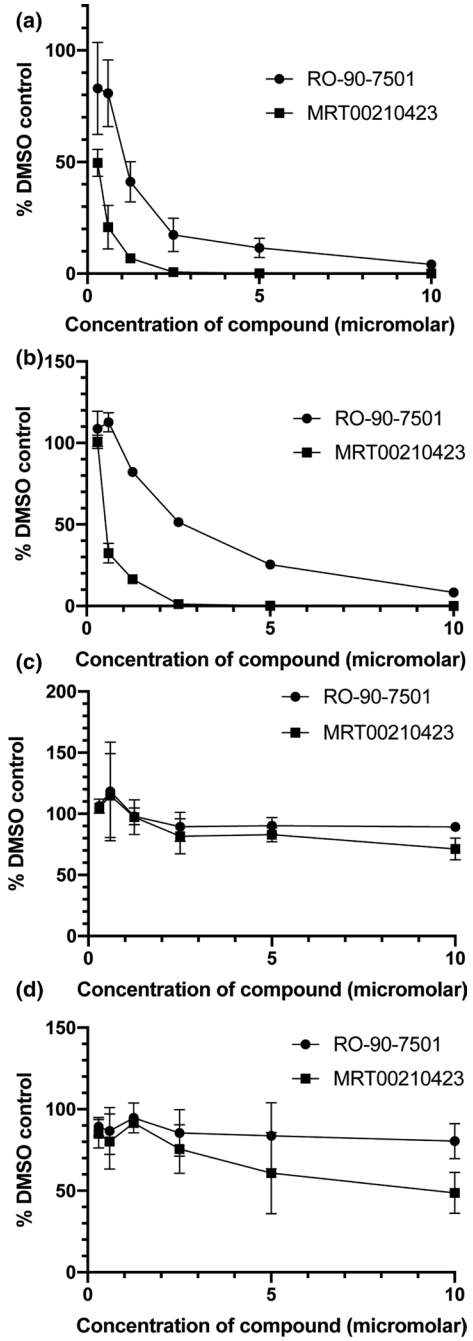

Fig. 4. Virus replication and toxicity in the presence of RO-90-7501 or MRT00210423. HFF cells were infected with HCMV strain (a) AD169 or (b) Merlin(R1111) and then treated with the concentrations of RO-90-7501 or MRT00210423 indicated in the figure or the corresponding volume of DMSO. Virus production at 96 h post-infection is shown as the percentage of infectious virus in the presence of RO-90-7501 or MRT00210423 compared to the appropriate DMSO control. The titre of the viruses analysed in these figures is shown in Fig. S2. (c, d) A high and low concentration of HFF cells (respectively, see Methods) were treated for 96 h with the concentrations of RO-90-7501 or MRT00210423 indicated in the figure or the corresponding volume of DMSO and then examined using an MTT assay. The data points and error bars in each panel represent the mean of three independent experiments and the SD of those experiments, respectively. At some data points, the error bars are too small to be represented on the figure.

a bisbenzimide compound and structurally similar to other well-known bisbenzimide compounds that bind DNA, such as the so-called 'Hoechst dyes', which bind in the minor groove of the DNA helix via interactions with adenine–thymine base pairs [40] and fluoresce upon exposure to UV light. A comparison of RO-90-7501's structure with that of a well-characterized Hoechst dye, Hoechst 33258, is shown in Fig. 2. Also indicated in Fig. 2 is the mechanism by which Hoechst 33258 binds to DNA, principally through hydrogen bonds between amine groups in the Hoechst 33258 compound and groups within purine bases of the minor groove of DNA [40] (red dotted lines, Fig. 2a) [40]. As RO-90-7501 had the essential structure required for DNA binding [40], we hypothesized that RO-90-7501 could interact with DNA using the same mechanism as Hoechst 33258 (red dotted lines, Fig. 2b). To our knowledge, there were no previous reports of HCMV replication inhibition by bisbenzimide compounds or any other compound known to bind to the minor groove of the DNA helix.

Before continuing further, we were concerned that bisbenzimide compounds may have off-target effects that affect cell viability in cell culture experiments or *in vivo*, probably due to their ability to bind DNA. However, it had been reported that Hoechst 33342 could inhibit poxvirus replication in cell culture experiments with no obvious cellular toxicity [41]. In addition, Hoechst 33342 has been administered to mice with no obvious adverse effects [42] and the bisbenzimide compound pibenzimol has been administered to humans without obvious adverse effects [43]. Therefore, we speculated that RO-90-7501 and similar compounds may not have off-target effects that would obviously limit their use in cell culture or *in vivo*.

Identification of RO-90-7501 analogues with anti-HCMV activity

Modification of compound structure can often reveal novel compounds with enhanced antiviral activity. Therefore, to find novel compounds with anti-HCMV activity, we generated compounds structurally related to RO-90-7501 (Fig. 3). As DNA binding is likely to be essential for the antiviral activity of RO-90-7501, we decided that any compounds we generated must contain the amine groups within RO-90-7501 that are likely to be required for DNA binding (highlighted in red, Fig. 3). It was unknown what, if any, effect the amine groups at the termini of RO-90-7501 had on anti-HCMV activity (highlighted in green, Fig. 3). Therefore, we focused on modifying the termini of RO-90-7501. We generated compounds that did not possess either of the terminal amine groups (MRT00210425 and MRT00210424) and a compound that had neither of the terminal amine groups (MRT00210423) (Fig. 3).

We compared the antiviral activity of these compounds to that of RO-90-7501 and DMSO (Fig. 3). MRT00210425, MRT00210424 and MRT00210423 all had anti-HCMV activity greater than that of RO-90-7501. Loss of either terminal amino group of RO-90-7501 (MRT00210425 and MRT00210424) had a moderately greater antiviral effect compared to RO-90-7501, whereas loss of both terminal amino groups (MRT00210423) showed the greatest antiviral effect compared to RO-90-7501.

We decided to focus our efforts on studying the antiviral effects of MRT00210423 compared to RO-90-7501.

Investigation of RO-90-7501 and MRT00210423 anti-HCMV activity

To confirm that RO-90-7501 and MRT00210423 could inhibit HCMV replication, a virus yield reduction assay was used to compare the production of HCMV strain AD169 in the presence of increasing concentrations of RO-90-7501, MRT00210423 or DMSO (Fig. 4a). We found a dose-dependent decrease in HCMV production in the presence of both RO-90-7501 and MRT00210423, indicating that both compounds were able to inhibit AD169 replication. The 50% effective concentration (EC_{50}) values of RO-90-7501 and MRT00210423 were calculated as 1.2 and 0.3 µM respectively. Consistent with the data shown in Fig. 3, the EC_{50} value of MRT00210423 was greater than that of RO-90-7501. We found similar results when we assayed the ability of RO-90-7501 to inhibit replication of the low-passage HCMV strain Merlin (Fig. 4b), whose genetic content was similar to wild-type strains of HCMV [35] (EC_{50} of 2.6 and 0.5 µM for RO-90-7501 and MRT00210423, respectively). Therefore, RO-90-7501 and MRT00210423 could inhibit HCMV replication and could do so at EC_{50} concentrations similar to those reported for the current frontline anti-HCMV drug ganciclovir [26, 44].

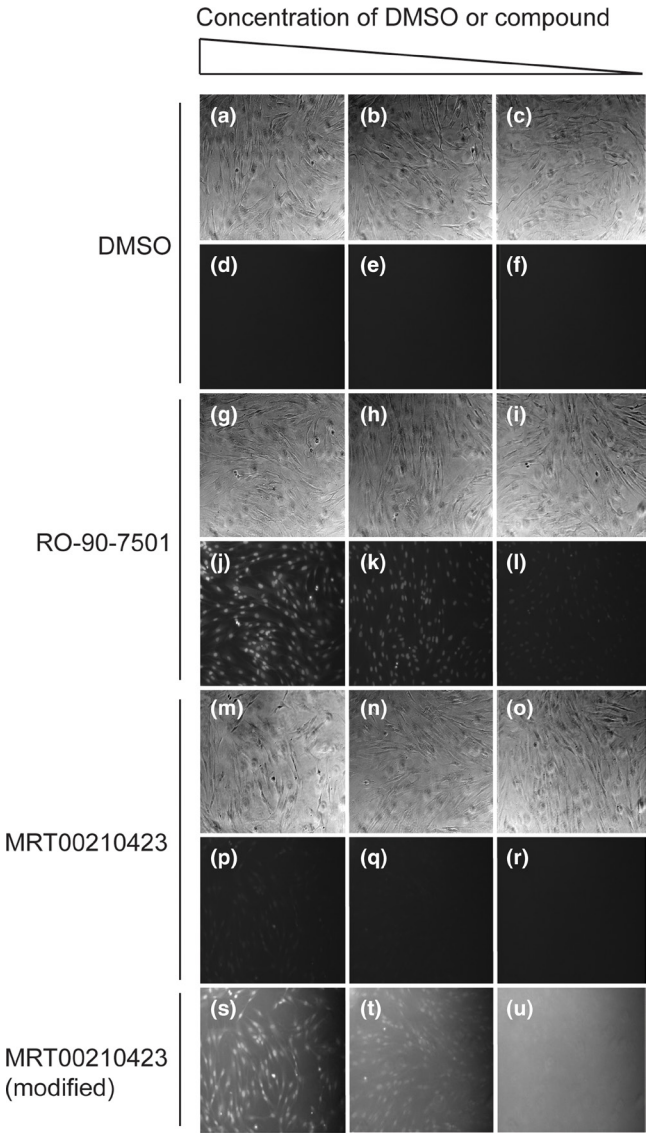

Fig. 5. Association of RO-90-7501 and MRT00210423 with host cell chromatin. HFF cells were treated with decreasing concentrations (10, 1, 0.1 µM, left to right in the figure) of RO-90-7501 or MRT00210423 or the equivalent volume of DMSO and examined by light microscopy. Brightfield (a–c, g–i, m–o) and UV emission images (d–f, j–l, p–r, s–u) are shown. In panels s–u images have been manipulated using Photoshop to increase the brightness of the UV emission from HFF cells treated with MRT00210423 (panels p–r).

We then used an MTT assay to assess the viability of a high concentration of uninfected cells treated with increasing concentrations of DMSO or RO-90-7501 (Fig. 4c). The 50% cellular toxicity concentration (CC_{50}) of both compounds was in excess of 10 µM, considerably greater than the EC_{50} values observed in Fig. 4(a). We also performed this assay with a low concentration of uninfected cells to assess both cell viability and proliferation (Fig. 4d). The CC_{50} concentration of both compounds was in excess of 10 µM. Therefore, treatment of cells with RO-90-7501 or MRT00210423 had no obvious toxic effect in either assay, and the inhibition of virus replication observed in our virus yield reduction assays (Fig. 4a, b) was unlikely to be due to toxic effects of either RO-90-7501 or MRT00210423.

Investigation of compound association with DNA

To confirm that RO-90-7501 and MRT00210423 could associate with DNA, we used light microscopy to understand if, like Hoechst compounds, RO-90-7501 and MRT00210423 could associate with host cell chromatin in uninfected cells. HFF cells were treated with either RO-90-7501, MRT00210423 or DMSO. Upon exposure to UV light, host cell chromatin could be visualized in cells treated with both RO-90-7501 and MRT00210423 (Fig. 5), suggesting that RO-90-7501 was associated with host cell chromatin. We noted that visualization of chromatin in cells treated with MRT00210423 was not as obvious as those cells treated with RO-90-7501. However, we hypothesized that this may have been due to differences in fluorescence emission of RO-90-7501 and MRT00210423 or a difference in the association of the compounds with chromatin. Treatment of cells with DMSO did not result in the ability to visualize host cell chromatin in cells (Fig. 5).

To confirm that our compounds interacted with DNA in the cell and not another factor in the cell nuclei, we also tested whether RO-90-7501 and MRT00210423 could associate with DNA outside of the cell. We have been unable to separate HCMV DNA from cellular DNA in infected cell lysate or recover high concentrations of intact HCMV genomes from preparations of HCMV virions (both data not

shown). Moreover, the size (over 230 kbp) and complexity of the HCMV genome meant that HCMV genomes could not be easily manipulated in biochemical assays. Therefore, for convenience, we assayed the ability of RO-90-7501 and MRT00210423 to interact with linear plasmid DNA (Fig. 6).

Biochemical studies of Hoechst 33258 in interaction with DNA have identified canonical DNA sequences to which bisbenzimide compounds are likely to preferentially bind [40, 45]. Further analysis of Hoechst 33258 binding to DNA revealed that bisbenzimide compounds are likely to have different affinities for these canonical DNA binding sites in cells [46]. In order of greatest to lowest affinity, bisbenzimide compounds are likely to bind to the canonical DNA sequences: AAATT, ATTTT, AATAA, TATA, TTAATG, GTTTAT and TTTCT [46]. To test compound binding to DNA we used a plasmid (pUC19) that contained several of the aforementioned sequences (Fig. 6a). We noted that these sequences are present in high quantity in the sequence of the HCMV AD169 (Fig. 6b and listed in Table S7). Also, the HCMV Merlin genome had a near identical number of each putative binding site in its genome, compared to the AD169 genome (listed in Table S8).

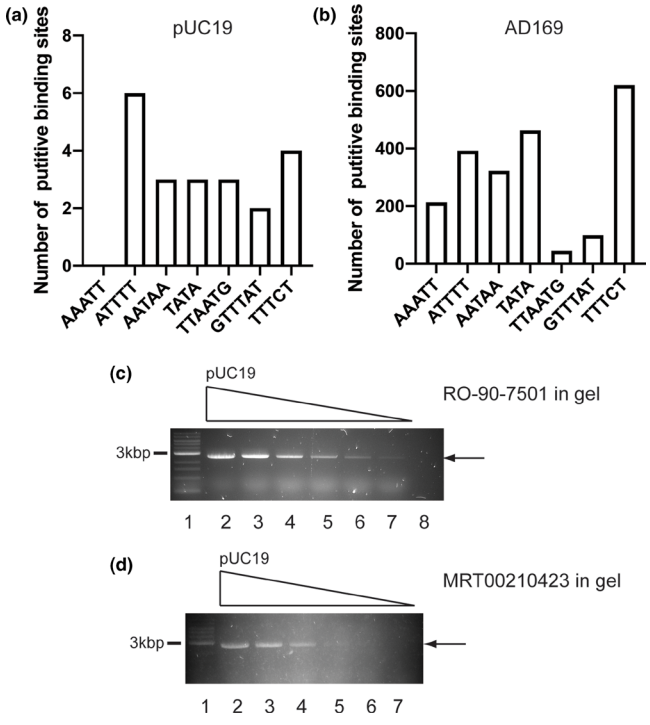

Fig. 6. Association of RO-90-7501 and MRT00210423 with plasmid DNA. (a,b) The number of putative compound binding sites in the sequence of pUC19 and the HCMV AD169 genome, respectively. (c) RO-90-7501 or (d) MRT00210423 was incorporated into agarose gels. Linear pUC19 plasmid (2.6 kbp) and a DNA molecular weight ladder were introduced into the gel via electrophoresis and the gel was subjected to UV radiation. In both panels: Lane 1, DNA molecular weight ladder, Lanes 2-onward, two-fold dilution series of 1 µg linear pUC19 plasmid. The position of pUC19 is indicated with an arrow to the right of each figure. The position of the 3 kbp marker in Lane 1 is indicated to the left of each figure.

Linear plasmid DNA was introduced into an agarose gel containing either RO-90-7501 or MRT00210423 using electrophoresis (Fig. 6c, d, respectively). Upon exposure of the gel to UV light, a DNA band corresponding to the expected molecular weight of the linear plasmid DNA was observed in both experiments, suggesting that RO-90-7501 and MRT00210423 were associated with plasmid DNA within the agarose gel. Again, we noted that visualization of DNA in the presence of MRT00210423 was less obvious than in the experiment using RO-90-7501. Incorporation of a volume of DMSO equivalent to that used in the aforementioned experiment into agarose gels did not result in the visualization of any DNA species (data not shown). Together, the data shown in Figs 5 and 6 confirmed that RO-90-7501 and MRT00210423 could associate with DNA.

To investigate the relationship between the ability of our compounds to bind DNA and anti-HCMV effects, we generated two further compounds, MRT00210426 and MRT00210427, which lacked either of the amine groups that were probably required for binding of bisbenzimide compounds to DNA [40] (Fig. 7, the methyl groups substituted for amine groups highlighted in red in MRT00210426 and MRT00210427) and studied the ability of these compounds to inhibit HCMV replication in virus replication assays (Fig. 7). Compared to treatment of cells with DMSO, we found that neither MRT00210426 nor MRT00210427 had any obvious anti-HCMV effect, whereas MRT00210423 demonstrated an anti-HCMV effect similar to that shown in Fig. 3. This indicated that an association of bisbenzimide compounds with DNA was necessary for anti-HCMV activity.

To confirm the relationship between anti-HCMV activity and DNA association of the aforementioned compounds, we then tested the ability of compounds to associate with DNA in agarose gels. A DNA molecular weight marker was introduced into an agarose gel containing compounds indicated in Fig. 7 using electrophoresis (Fig. S3). Gels were then photographed upon exposure to UV light, then washed in the UV light-sensitive DNA stain SYBR Green and again exposed to UV light and photographed. We found that DNA could be observed in gel containing MRT00210423 upon initial exposure to UV light. However, DNA could only be visualized in gels containing MRT00210426 or MRT00210427 only after the gels were washed with the DNA stain SYBR Green. These data suggested that MRT00210423 was associated with DNA in the agarose gel, but MRT00210426 and MRT00210427 were not. Therefore, there was a relationship between the ability of compounds to associate with DNA and anti-HCMV effects. Furthermore, the binding of our compounds to host cell chromatin (Fig. 5) and presence of putative bisbenzimide compound binding sites in the HCMV genome (Fig. 6) suggested that our compounds may have bound to both host cell chromatin and the HCMV genome in infected cells.

Analysis of bisbenzimide action on DNA using single molecule microscopy

We then attempted to understand what effect RO-90-7501 and MRT00210423 might have on DNA in HCMV-infected cells. It has been reported that binding of bisbenzimide compounds to DNA can result in compaction of DNA via condensation of the DNA helix [47], which could inhibit any number of biological processes. We therefore used a single molecule flow-stretching technique to analyse compaction of a DNA substrate in the presence of our bisbenzimide compounds. In this assay a bacteriophage lambda genome (which contains 479 bisbenzimide binding sites) labelled with a quantum dot was placed within a microfluidic flow cell into which buffer could flow. Using total internal reflection fluorescence microscopy, the positions of a quantum dot were tracked in real time while the DNA was stretched by buffer flow. Quantum dot movement in the presence of flow away or towards the tether could be interpreted to understand elongation or compaction of the bacteriophage DNA, respectively (Fig. 8a).

We conducted a series of preliminary experiments in which increasing concentrations of RO-90-7501 or MRT00210423 were flowed into a microfluidic flow cell. We found that increasing concentrations of RO-90-7501 appeared to quench emission from the quantum dots used. The same was found in the presence of MRT00210423, albeit to apparently a lesser extent. Therefore, we assayed quantum dot movement at a minimum concentration of RO-90-7501 in which the quantum dots could be readily visualized while any change in quantum dot movement was observed. Therefore, we flowed the volume of DMSO equivalent to 75 µM of either compound resuspended in DMSO into a flow cell and found that the quantum dot visualized did not obviously move in the buffer flow (Fig. 8b). However, when a concentration of 75 µM RO-90-7501 was then flowed into a flow cell, emission from the quantum dot decreased over time and the quantum dot moved against the direction of buffer flow (Fig. 8c). However, when 75 µM MRT00210423 was added to a flow cell there was no obvious movement of the quantum dot (Fig. 8d). To ensure that the lack of MRT00210423 compaction in this assay was not due to a concentration-dependent effect, we repeated the assay adding increasing concentrations of MRT00201423 up to 1 mM. However, we observed no compaction of DNA in the presence of MRT00210423 at any of the compound concentrations tested (data not shown).

Therefore, RO-90-7501 was able to compact DNA in this assay, whereas MRT00210423 did not. This suggested that compaction of DNA in HCMV-infected cells was not obligatory for anti-HCMV effects and binding of compounds to DNA alone was sufficient for our compounds to exert anti-HCMV effects.

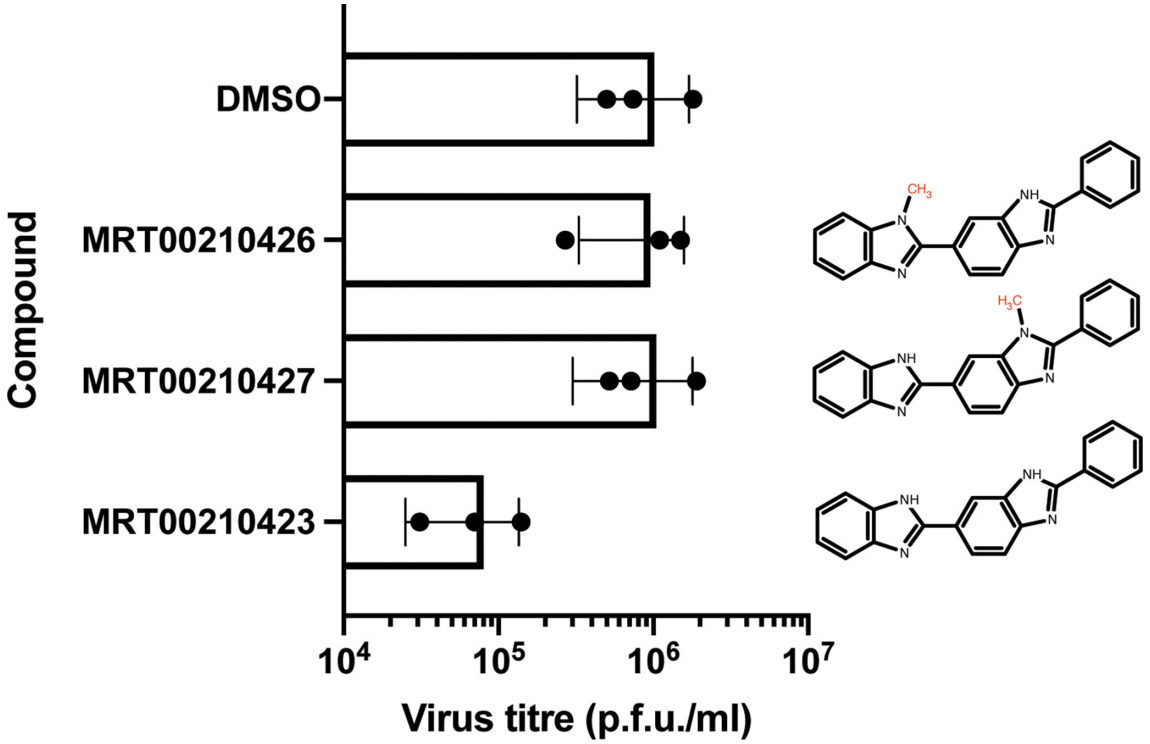

Fig. 7. Investigation of anti-HCMV activity of MRT00210423 analogues and their association with DNA. (a) HFF cells were infected with HCMV strain AD169 (m.o.i. 1) in the presence of the compounds indicated in the figure (1 µM) or an equivalent volume of DMSO. At 96 h post-infection virus titre (p.f.u. ml^{-1}) from these infections was determined. The data points from three independent experiments are shown. The columns and error bars represent the mean and SD, respectively, of those data points. The structures of the bisbenzimide compounds examined are shown to the right of the figure. The methyl groups substituted for amine groups are highlighted in red in MRT00210426 and MRT00210427.

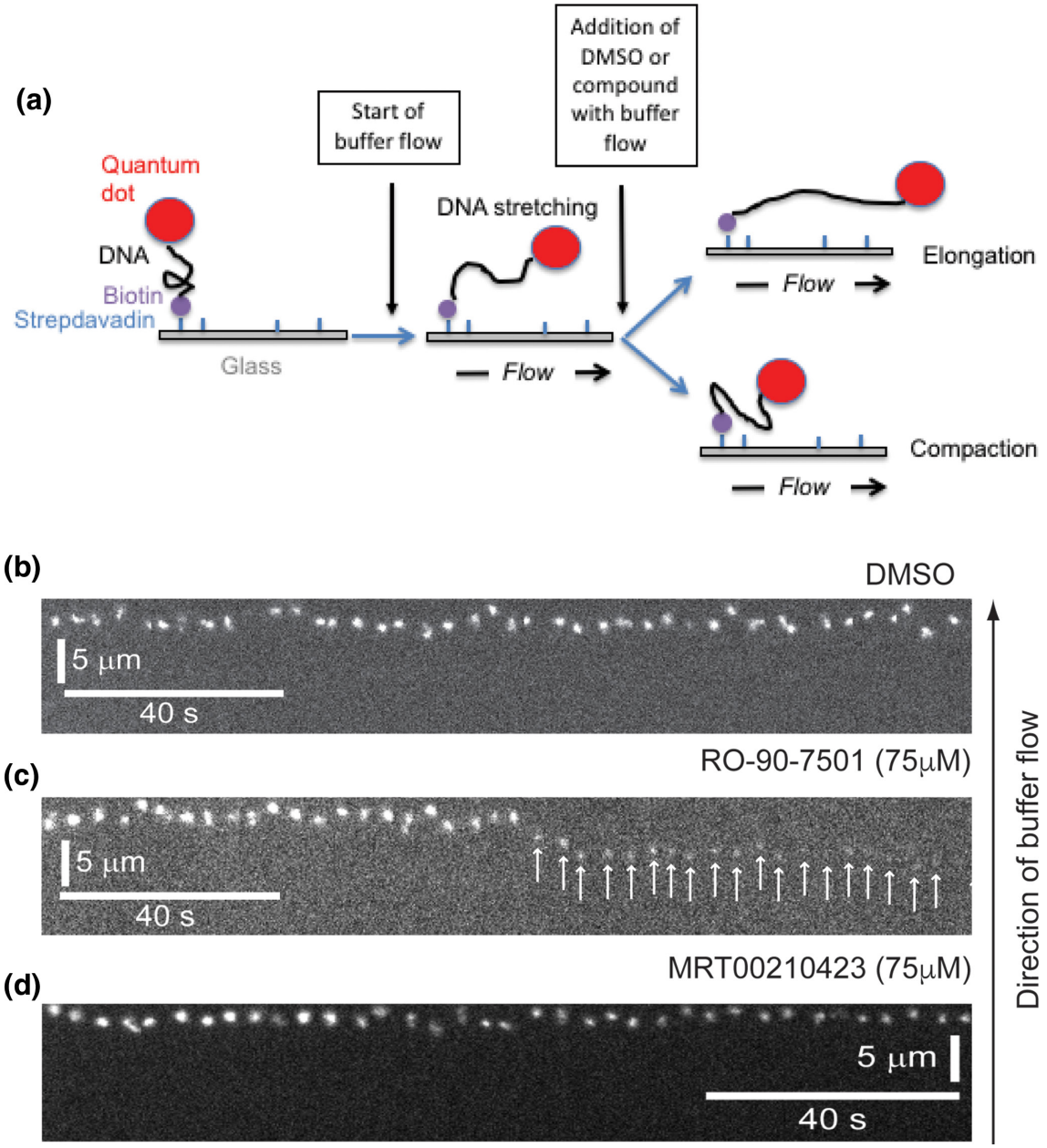

Fig. 8. Single molecule imaging of a quantum dot in the presence of RO-90-7501 or MRT00210423. A schematic of the experiment is shown in (a). A microscopy flow cell containing bacteriophage lambda DNA conjugated with a quantum dot was prepared as described in the Methods. Buffer containing (b) a volume of DMSO equivalent to 75 µM or either compound (c) 75 µM RO-90-7501 or (d) 75 µM MRT00210423 was flowed into the microscopy flow cell and movement of the quantum dot was recorded using a total internal reflection fluorescence microscope. Kymograph panels (b)–(d) show sequential images of the quantum dot in buffer containing either DMSO, RO-90-7501 or MRT00210423 over time. The time frame of the images and the distance are represented with horizontal and vertical bars, respectively, in each panel. The direction of the buffer flowing into the microscopy cell is shown with an arrow. In (c) arrows are used to shown the position of the quantum dot.

Investigation of HCMV replication in HCMV-infected cells treated with bisbenzimide compounds

We then sought to understand how RO-90-7501 and MRT00210423 inhibited HCMV replication in infected cells. First, we investigated HCMV protein production to understand at what point in HCMV replication our compounds acted. A hallmark of HCMV replication is the production of proteins via a transcriptional cascade of immediate-early, early and late transcription. Using western blotting, we assayed the production of proteins representative of all three classes of viral transcription [HCMV transcriptional transactivators IE1/IE2 representing proteins produced via

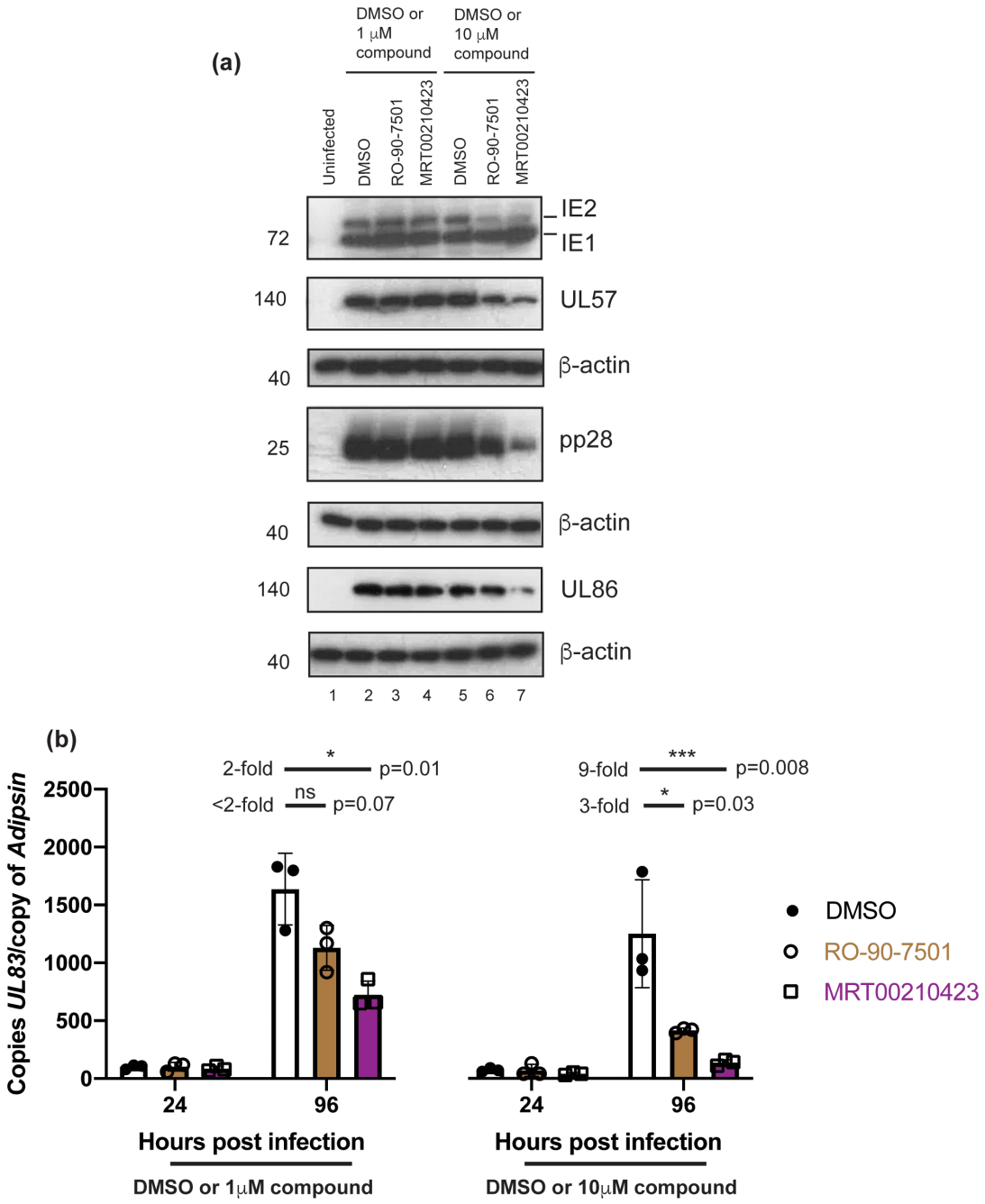

Fig. 9. Production of HCMV proteins, DNA and capsids in the presence of bisbenzimide compounds. (a) HFF cells were infected with HCMV strain AD169 and treated with the concentrations of RO-90-7501, MRT00210423 (both in 2-fold dilution series starting at 10 μM) or the corresponding volumes of DMSO. Cell lysates were prepared for western blotting at 72 h post-infection. Western blotting was used to detect viral (IE1/IE2, UL57 and pp28) and cellular (*β*-actin) proteins in infected cells treated with either DMSO (lanes 2 and 5), RO-90-7501 (lanes 3 and 6) or MRT00210423 (lanes 4 and 7). Uninfected cells were harvested for analysis at the time of infection (lane 1). Proteins recognized by the antibodies used are indicated to the right of each figure. The positions of molecular mass markers (kDa) are indicated to the left of each figure. Blots for IE1/IE2 and UL57 or pp28 or UL86 were performed on separate gels. (b) Viral DNA synthesis was determined by quantitative real-time PCR analysis of DNA prepared from infected HFF cell lysate (AD169, m.o.i. 1, in the presence of 1 or 10 μM compound or the equivalent volume of DMSO) prepared at the time points indicated in the figure. The amount of viral DNA detected was represented as copies of the viral gene *UL83* per copy of the cellular *adipsin* gene. The data points from three independent experiments are shown. The columns and error bars represent the mean and SD, respectively, of those data points. Statistical significance was assayed using an unpaired *t*-test and two-tailed *P* values are shown in the figure. The fold difference between the values of the mean data is also noted above the figure.

immediate-early transcription, HCMV DNA binding protein UL57 representing proteins produced via early transcription, HCMV virion protein pp28 (tegument protein) and UL86 (major capsid protein) representing proteins produced via late transcription] in the presence of either DMSO, RO-90-7501 or MRT00210423 (Fig. 9a). We found no obvious differences in the production of any viral protein in the presence of 1 μM RO-90-7501 or MRT00210423, compared to viral protein production in the presence of DMSO. However, compared to viral protein production in the presence of DMSO, there was a decrease in expression of some viral proteins in the presence of 10 μM RO-90-7501 and/or MRT00210423.

We then assayed synthesis of HCMV DNA using a quantitative PCR methodology (Fig. 9b). We assayed the number of viral DNA sequences compared to the number of a cellular DNA sequence that could be found in HCMV infected cells treated with either DMSO, RO-90-7501 or MRT00210423 (1 or 10 μM) at immediate-early (24 h post-infection) and late (96 h post-infection) time points. Compared to viral DNA synthesis in the presence of DMSO, we found that the presence of 1 μM RO-90-7501 or MRT00210423 had little effect on viral DNA synthesis, whereas the presence of 10 μM RO-90-7501 or MRT00210423 had a greater effect on viral DNA synthesis (Fig. 9b).

Therefore, the presence of 10 μM RO-90-7501 or MRT00210423 was sufficient to inhibit HCMV replication, HCMV protein production and DNA synthesis (Figs 4 and 9). However, the presence of 1 μM RO-90-7501 or MRT00210423 was sufficient to inhibit HCMV replication (Fig. 4), but was not sufficient to obviously inhibit either viral protein production or viral DNA synthesis (Fig. 9). Therefore, we speculated that there was a mechanism by which our compounds inhibited HCMV replication that did not involve inhibition of HCMV protein production or DNA synthesis. Packaging of nascent viral DNA into capsids in the nucleus is essential for HCMV replication. We hypothesized that our compounds may have interacted with newly synthesized HCMV DNA in the nucleus and prevented HCMV DNA packaging into capsids. To investigate this, we use electron microscopy of cells infected with HCMV in the presence of either DMSO or 1 or 10 μM of our compounds. We counted the number of each of the three capsid forms that can be found in HCMV-infected nuclei (A capsids, non-productive forms thought to result from failed packaging of viral genomes; B capsids, productive intermediates that contain a scaffolding protein; and C capsids, assembled forms in which the scaffolding protein has been removed and replaced with viral DNA) under each condition (Fig. 10). We anticipated that the presence of our compounds might alter the ratio of B (empty) to C (DNA-containing) capsids found in infected nuclei, indicating a defect in genome packaging into capsids. Surprisingly, while we observed large numbers of B capsids and smaller numbers of A and C capsids in the presence of DMSO, we found little or no of any capsid type in cells treated with either compound. Therefore, in the presence of 1 μM of our compounds, inhibition of HCMV replication was associated with lack of HCMV capsid production (Fig. 10), but not inhibition of production of HCMV proteins analysed (including the major capsid protein UL86, Fig. 9a) or inhibition of viral DNA synthesis (Fig. 9b). However in the presence of 10 μM of our compounds, inhibition of HCMV capsid production (Fig. 10) may have contributed to inhibition of HCMV replication and was associated with inhibition of production of HCMV proteins analysed (including the major capsid protein UL86, Fig. 9a) and viral DNA synthesis (Fig. 9b).

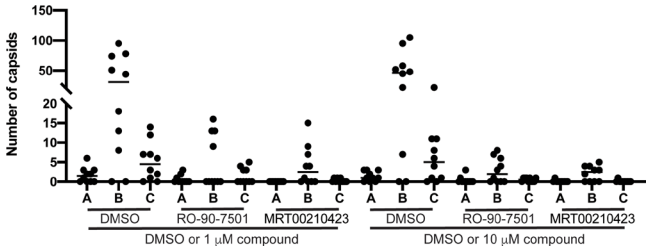

Fig. 10. Production of HCMV capsids in the presence of bisbenzimide compounds. Infected cells from three independent experiments [HFF cells infected with AD169 (m.o.i. 1) for 96 h in the presence of 1 or 10 μM of either compound, or the equivalent volume of DMSO] were combined and prepared for analysis by electron microscopy. In each condition, the number of A, B and C capsids in 10 nucleus profiles selected at random were counted. Only nuclei where the entire area of the nuclei could be visualized were counted.

DISCUSSION

We sought to increase the number of compounds available for inhibition of HCMV replication by screening collections of bioactive compounds. Our screening experiments identified a number of compounds not previously reported to inhibit HCMV replication. We chose to study RO-90-7501, whose mechanism of action was likely to be different from known anti-HCMV compounds. A key step in our studies was to discover an analogue of RO-90-7501, MRT00210423, which we found had greater anti-HCMV activity than RO-90-7501. We found that both RO-90-7501 and MRT00210423 had efficient anti-HCMV activity, with no obvious cellular toxicity, and that the antiviral activity of the compounds was probably due to their ability to interact with DNA. Interestingly, we found that RO-90-7501 and MRT00210423 had different effects on DNA. Surprisingly, we observed an association between the presence of compounds in infected cells and inhibition of HCMV capsid production.

We considered why MRT00210423 had greater anti-HCMV activity than RO-90-7501. Based upon an atomic structure of Hoechst 33258 binding to DNA, we reasoned it was possible that MRT00210423 may have had a greater ability to access the minor groove of DNA compared to RO-90-7501. The fit of Hoechst 33258 into the minor grove of the DNA was reported to be very close-fitting, with Hoechst 33258 occupying the entire volume of the DNA minor groove [40]. Binding of Hoechst 33258 to DNA [40] involved a twist in the Hoechst 33258 structure, and the arrangement of groups that comprise Hoechst 33258 was

not co-planar. Specifically, there was a small angle between the phenoic ring and the first benzimidazole group and a much larger angle between the two consecutive benzimidazole groups of the compound. The piperazine group was almost co-planar with the neighbouring benzimidazole group. Together, these data inferred that Hoechst 33258 had to be fitted into the minor groove of DNA [40]. Therefore, we propose that removal of the terminal amine groups from RO-90-7501 allowed a greater flexibility between the groups that comprise MRT00210423 and allowed a more efficient fit of MRT00210423 into the minor DNA groove and, thus, easier binding to DNA of MRT00210423 compared to RO-90-7501.

It was also possible that there were differences in metabolism of RO-90-7501 and MRT00210423 within the cell that resulted in differences in anti-HCMV activity between the two compounds. However, the structure of the two compounds was similar. Therefore, it was not obvious what these differences in metabolism might have been.

At a low concentration of our compounds we observed an association between inhibition of HCMV replication and a lack of HCMV capsid production. At present, it is unknown what molecular mechanisms our compounds use to prevent HCMV capsid production. Indeed, it is unclear or unknown how many aspects of capsid formation take place, including what viral and cellular factors are required for capsid formation and how these factors are localized and organized in infected cell nuclei. It is possible that our compounds had effects on one or several viral and cellular factors required for capsid formation. Furthermore, at a high concentration of our compounds we also found inhibition of HCMV capsid production. However, this could have been linked to defects we observed in HCMV protein production and viral DNA synthesis in the presence of a high concentration of our compounds. It is unknown if at a high concentration our compounds act on gene expression or protein production of the viral factors assayed in our experiments. That said, as we see efficient inhibition of HCMV replication at a low concentration of our compounds, investigation of our compounds at a high concentration is not a priority and future work should focus on the surprising observation that links inhibition of HCMV replication with lack of capsid production.

We hypothesized that our compounds would interact with HCMV DNA. However, at a low concentration of our compounds we observed little or no defect in HCMV DNA synthesis or production of those HCMV proteins analysed. This might suggest that our compounds did not act directly on HCMV DNA, but we cannot exclude the possibility that compound binding to the viral genome affected production of capsids via an as yet unknown mechanism. Interestingly, we have found obvious interaction of both compounds with chromatin in uninfected cells. Therefore, it was possible that binding of our compounds to cellular chromatin was required for anti-HCMV effects. As production of those HCMV proteins analysed and DNA synthesis were not obviously compromised by our compounds, it is unlikely that the interaction of our compounds with chromatin affected the formation of nuclear HCMV replication compartments, within which HCMV DNA synthesis occurs [48]. Rather, we propose that binding of our compounds to chromatin may have affected the production of one or many cellular factors required for HCMV replication. Of course, it is possible that the anti-HCMV effects of our compounds were due to compound binding to both viral DNA and chromatin. We considered if a mechanism other than compound binding to DNA was responsible for anti-HCMV effects. It should be noted that RO-90-7501 has been reported to enhance transcription from the β-IFN promoter upon induction of transcription using poly I:C [49]. However, we found no evidence for the ability of RO-90-7501 to enhance β-IFN production in HCMV-infected cells (data not shown) and the aforementioned work did not investigate what, if any, effects interaction of RO-90-7501 with chromatin had on enhancing transcription from the β-IFN promoter [49].

It is also interesting to consider the mechanistic details of how compound binding to DNA resulted in anti-HCMV effects. We hypothesized that, like other bisbenzimide compounds [47], binding of our compounds to DNA would result in DNA compaction. DNA compaction could have multiple effects on DNA function. However, we found compaction of DNA in the presence of RO-90-7501, but not MRT00210423. Therefore, compaction of DNA for anti-HCMV effects was non-obligatory and binding of compounds to DNA alone may have been sufficient for anti-HCMV effects.

That said, RO-90-7501 and MRT00210423 could be useful tools in biochemical studies of DNA compaction and its biological effects. It is possible that DNA compaction by RO-90-7501 resulted in the formation of non-specific structures in DNA and/or loop formation by bridging two different segments of a DNA. Looping of DNA was consistent with the relatively long distance travelled by DNA in our single molecule DNA stretching experiments in the presence of RO-90-7501. The underlying mechanisms of DNA looping are largely unknown, but important for essential biological processes. Comparing how our compounds bind to DNA and how they have different effects could further our understanding of DNA function in the cell.

For future development of compounds for clinical use it may be necessary to find compounds related to RO-90-7501 and MRT00210423 that bind preferentially to HCMV genomes compared to host cell chromatin. Bisbenzimide compounds are amenable to a range of medicinal chemistry approaches (for examples see references [50–55]). These could lead to identification of analogues of our compounds that preferentially bind HCMV genomes or the conjugation of our compounds to DNA-binding proteins to target the compound to HCMV DNA.

That said, several factors support further development of RO-90-7501 or MRT00210423 as anti-HCMV compounds. Current anti-HCMV therapy can be limited by drug resistance [7–12]. As yet, we have not been able to generate HCMV viruses resistant to either RO-90-7501 or MRT00210423 (data not shown). Plus, as mentioned above, it has been reported that administration of bisbenzimide compounds has had no serious adverse effects in murine model experiments and clinical trials

in humans [42, 43]. Finally, RO-90-7501 and MRT00210423 or related compounds could have broad antiviral activity, as it has been demonstrated that bisbenzimide compounds have antiviral activity against poxviruses [41] and RO-90-7501 can inhibit replication of vesicular stomatitis virus [49], a model virus for many important Rhabdoviruses affecting human health.

Funding information
This work was supported by New Investigator funds from St George's, University of London, St George's Impact & Innovation Awards (2014 and 2018), a PARK/WestFocus Award, MRC Industrial CASE studentship MR/M016226/1 (all to B.L.S.), plus the University of Texas Rio Grande Valley Start-up Grant and the University of Texas System's Rising STARs Award (both to H.J.K.). We are grateful to Don Coen (Harvard Medical School) for his support of B.L.S. during the screening experiments featured here via grants awarded to D.C. from the National Institutes of Health (R01 AI019838 and R01 AI026077).

Acknowledgements
We are grateful to Don Coen for his encouragement during this study and his support of B.L.S. during the screening experiments. We also acknowledge Don Coen, Steve Goodbourn, Richard Stanton and Wade Gibson for kindly providing reagents. For assistance with light and electron microscopy we thank Greg Perry and all other members of the SGUL Image Resource Facility. Thanks, also, to Lucy Collinson (Science Technology Platform, Francis Crick Institute) for assistance with electron microscopy. We thank Steve Goodbourn and Jason Mercer for valuable discussions. Special thanks go to all members of the Institute of Chemistry and Chemical Biology-Longwood for their assistance in all aspects of the compound screening process.

Author contributions
N.F.F.: Investigation, Methodology, Formal Analysis, Writing-Review and Editing. H.J.K.: Investigation, Methodology, Formal Analysis. L.Z.H.: Investigation. M.R.G.R.: Investigation, Methodology. C.M-K.H.: Investigation, Methodology. V.B.S.: Investigation, Methodology. H.A.W.: Methodology. A.M.: Conceptualization, Methodology, Formal Analysis, Data Curation Resources, Supervision, Funding. B.L.S.: Conceptualization, Investigation, Methodology, Formal Analysis, Data Curation, Resources, Writing-Original Draft Preparation, Writing-Review and Editing, Supervision, Project Administration, Funding.

Conflicts of interest
The authors declare there are no conflicts of interest.

References

1. Griffiths PD. Burden of disease associated with human cytomegalovirus and prospects for elimination by universal immunisation. *Lancet Infect Dis* 2012;12.
2. Krause PR, Bialek SR, Boppana SB, Griffiths PD, Laughlin CA, *et al*. Priorities for CMV vaccine development. *Vaccine* 2013;32:4–10.
3. Coen DM, Schaffer PA. Antiherpesvirus drugs: a promising spectrum of new drugs and drug targets. *Nat Rev Drug Discov* 2003;2:278–288.
4. Lischka P, Hewlett G, Wunberg T, Baumeister J, Paulsen D, *et al*. *In vitro* and *in vivo* activities of the novel anticytomegalovirus compound AIC246. *Antimicrob Agents Chemother* 2010;54:1290–1297.
5. Biron KK, Harvey RJ, Chamberlain SC, Good SS, Smith AA, *et al*. Potent and selective inhibition of human cytomegalovirus replication by 1263W94, a benzimidazole l -riboside with a unique mode of action. *Antimicrob Agents Chemother* 2002;46:2365–2372.
6. Goldner T, Hewlett G, Ettischer N, Ruebsamen-Schaeff H, Zimmermann H, *et al*. The novel anticytomegalovirus compound AIC246 (Letermovir) inhibits human cytomegalovirus replication through a specific antiviral mechanism that involves the viral terminase. *J Virol* 2011;85:10884–10893.
7. Chou S. A third component of the human cytomegalovirus terminase complex is involved in letermovir resistance. *Antiviral Res* 2017;148:1–4.
8. Cherrier L, Nasar A, Goodlet KJ, Nailor MD, Tokman S, *et al*. Emergence of letermovir resistance in a lung transplant recipient with ganciclovir-resistant cytomegalovirus infection. *Am J Transplant* 2018;18:3060–3064.
9. Chou S, Satterwhite LE, Ercolani RJ. New locus of drug resistance in the human cytomegalovirus UL56 gene revealed by *in vitro* exposure to letermovir and ganciclovir. *Antimicrob Agents Chemother* 2018;62.
10. Chou S. Rapid *in vitro* evolution of human cytomegalovirus UL56 mutations that confer letermovir resistance. *Antimicrob Agents Chemother* 2015;59:6588–6593.
11. Chou S, Wechel LCV, Marousek GI. Cytomegalovirus UL97 kinase mutations that confer maribavir resistance. *J Infect Dis* 2007;196:91–94.
12. Papanicolaou GA, Silveira FP, Langston AA, Pereira MR, Avery RK, *et al*. Maribavir for refractory or resistant cytomegalovirus infections in hematopoietic-cell or solid-organ transplant recipients: a randomized, dose-ranging, double-blind, phase 2 study. *Clin Infect Dis* 2019;68:1255–1264.
13. Marty FM, Ljungman P, Papanicolaou GA, Winston DJ, Chemaly RF, *et al*. Maribavir prophylaxis for prevention of cytomegalovirus disease in recipients of allogeneic stem-cell transplants: a phase 3, double-blind, placebo-controlled, randomised trial. *Lancet Infect Dis* 2011;11:284–292.
14. Marty FM, Boeckh M. Maribavir and human cytomegalovirus-what happened in the clinical trials and why might the drug have failed? *Curr Opin Virol* 2011;1:555–562.
15. Mocarski ES, Shenk T, Griffiths PD, Pass RF. Cytomegaloviruses. In: Knipe DM and Howley PM (eds). *Fields Virology*, 6th edn, vol. 2. New York, NY: Lippincott, Williams & Wilkins; 2015. pp. 1960–2015.
16. Mercorelli B, Luganini A, Nannetti G, Tabarrini O, Palù G, *et al*. Drug repurposing approach identifies inhibitors of the prototypic viral transcription factor IE2 that block human cytomegalovirus replication. *Cell Chem Biol* 2016;23.
17. Gardner TJ, Cohen T, Redmann V, Lau Z, Felsenfeld D, *et al*. Development of a high-content screen for the identification of inhibitors directed against the early steps of the cytomegalovirus infectious cycle. *Antiviral Res* 2015;113:49–61.
18. Nukui M, O'Connor CM, Murphy EA. The natural flavonoid compound deguelin inhibits HCMV lytic replication within fibroblasts. *Viruses* 2018;10:E614.
19. Mukhopadhyay R, Roy S, Venkatadri R, Su Y-P, Ye W, *et al*. Efficacy and mechanism of action of low dose emetine against human cytomegalovirus. *PLoS Pathog* 2016;12:e1005717.
20. Strang BL. RO0504985 is an inhibitor of CMGC kinase proteins and has anti-human cytomegalovirus activity. *Antiviral Res* 2017;144:21–26.
21. Khan AS, Murray MJ, Ho CMK, Zuercher WJ, Reeves MB, *et al*. High-throughput screening of a GlaxoSmithKline protein kinase inhibitor set identifies an inhibitor of human cytomegalovirus replication that prevents CREB and histone H3 post-translational modification. *J Gen Virol* 2017;98:754–768.
22. Beelontally R, Wilkie GS, Lau B, Goodmaker CJ, Ho CMK, *et al*. Identification of compounds with anti-human cytomegalovirus activity that inhibit production of IE2 proteins. *Antiviral Res* 2017;138:61–67.
23. Polachek WS, Moshrif HF, Franti M, Coen DM, Sreenu VB, *et al*. High-throughput small interfering RNA screening identifies phosphatidylinositol 3-kinase class II alpha as important for production of human cytomegalovirus virions. *J Virol* 2016;90:8360–8371.
24. Birmingham A, Selfors LM, Forster T, Wrobel D, Kennedy CJ, *et al*. Statistical methods for analysis of high-throughput RNA interference screens. *Nat Methods* 2009;6:569–575.
25. Zhang JH, Chung TD, Oldenburg KR. A simple statistical parameter for use in evaluation and validation of high throughput screening assays. *J Biomol Screen* 1999;4:67–73.
26. Loregian A, Coen DM. Selective anti-cytomegalovirus compounds discovered by screening for inhibitors of subunit interactions of the viral polymerase. *Chem Biol* 2006;13:191–200.

27. Kim H, Loparo JJ. Observing bacterial chromatin protein-DNA interactions by combining DNA flow-stretching with single-molecule imaging. *Methods Mol Biol* 2018;1837:277–299.
28. Kim H, Loparo JJ. Multistep assembly of DNA condensation clusters by SMC. *Nat Commun* 2016;7:10200.
29. Edelstein AD, Tsuchida MA, Amodaj N, Pinkard H, Vale RD, *et al*. Advanced methods of microscope control using μManager software. *J Biol Methods* 2014;1:e10.
30. Schneider CA, Rasband WS, Eliceiri KW. NIH Image to ImageJ: 25 years of image analysis. *Nat Methods* 2012;9:671–675.
31. Strang BL, Stow ND. Circularization of the herpes simplex virus type 1 genome upon lytic infection. *J Virol* 2005;79:12487–12494.
32. Strang BL, Bender BJ, Sharma M, Pesola JM, Sanders RL, *et al*. A mutation deleting sequences encoding the amino terminus of human cytomegalovirus UL84 impairs interaction with UL44 and capsid localization. *J Virol* 2012;86:11066–11077.
33. Strang BL, Boulant S, Kirchhausen T, Coen DM, Sandri-Goldin RM. Host cell nucleolin is required to maintain the architecture of human cytomegalovirus replication compartments. *mbio* 2012;3.
34. Kremer JR, Mastronarde DN, McIntosh JR. Computer visualization of three-dimensional image data using IMOD. *J Struct Biol* 1996;116:71–76.
35. Wilkinson GWG, Davison AJ, Tomasec P, Fielding CA, Aicheler R, *et al*. Human cytomegalovirus: taking the strain. *Med Microbiol Immunol* 2015;204:273–284.
36. Britt WJ, Jarvis M, Seo JY, Drummond D, Nelson J. Rapid genetic engineering of human cytomegalovirus by using a lambda phage linear recombination system: demonstration that pp28 (UL99) is essential for production of infectious virus. *J Virol* 2004;78:539–543.
37. Depto AS, Stenberg RM. Functional analysis of the true late human cytomegalovirus pp28 upstream promoter: cis-acting elements and viral trans-acting proteins necessary for promoter activation. *J Virol* 1992;66:3241–3246.
38. De Clercq E, Sakuma T, Baba M, Pauwels R, Balzarini J, *et al*. Antiviral activity of phosphonylmethoxyalkyl derivatives of purine and pyrimidines. *Antiviral Res* 1987;8:261–272.
39. Elion GB. Mechanism of action and selectivity of acyclovir. *Am J Med* 1982;73:7–13.
40. Teng MK, Usman N, Frederick CA, Wang AH. The molecular structure of the complex of Hoechst 33258 and the DNA dodecamer d(CGCGAATTCGCG). *Nucleic Acids Res* 1988;16:2671–2690.
41. Yakimovich A, Huttunen M, Zehnder B, Coulter LJ, Gould V, *et al*. Inhibition of poxvirus gene expression and genome replication by bisbenzimide derivatives. *J Virol* 2017;91:18.
42. Olive PL, Chaplin DJ, Durand RE. Pharmacokinetics, binding and distribution of Hoechst 33342 in spheroids and murine tumours. *Br J Cancer* 1985;52:739–746.
43. Patel SR, Kvols LK, Rubin J, O'Connell MJ, Edmonson JH, *et al*. Phase I-II study of pibenzimol hydrochloride (NSC 322921) in advanced pancreatic carcinoma. *Invest New Drugs* 1991;9:53–57.
44. Faulds D, Heel RC. Ganciclovir. A review of its antiviral activity, pharmacokinetic properties and therapeutic efficacy in cytomegalovirus infections. *Drugs* 1990;39:597–638.
45. Harshman KD, Dervan PB. Molecular recognition of B-DNA by Hoechst 33258. *Nucleic Acids Res* 1985;13:4825–4835.
46. Hampshire AJ, Fox KR. The effects of local DNA sequence on the interaction of ligands with their preferred binding sites. *Biochimie* 2008;90:988–998.
47. Saito M, Kobayashi M, Iwabuchi S, Morita Y, Takamura Y, *et al*. DNA condensation monitoring after interaction with hoechst 33258 by atomic force microscopy and fluorescence spectroscopy. *J Biochem* 2004;136:813–823.
48. Strang BL, Boulant S, Chang L, Knipe DM, Kirchhausen T, *et al*. Human cytomegalovirus UL44 concentrates at the periphery of replication compartments, the site of viral DNA synthesis. *J Virol* 2012;86:2089–2095.
49. Guo F, Mead J, Aliya N, Wang L, Cuconati A, *et al*. RO 90-7501 enhances TLR3 and RLR agonist induced antiviral response. *PloS one* 2012;7:e42583.
50. Bathini Y, Rao KE, Shea RG, Lown JW. Molecular recognition between ligands and nucleic acids: novel pyridine- and benzoxazole-containing agents related to Hoechst 33258 that exhibit altered DNA sequence specificity deduced from footprinting analysis and spectroscopic studies. *Chem Res Toxicol* 1990;3:268–280.
51. Guan LL, Zhao R, Lown JW. Enhanced DNA alkylation activities of Hoechst 33258 analogues designed for bioreductive activation. *Biochem Biophys Res Commun* 1997;231:94–98.
52. Gupta R, Wang H, Huang L, Lown JW. Design, synthesis, DNA sequence preferential alkylation and biological evaluation of N-mustard derivatives of Hoechst 33258 analogues. *Anticancer Drug Des* 1995;10:25–41.
53. Kumar S, Yadagiri B, Zimmermann J, Pon RT, Lown JW. Sequence specific molecular recognition and binding by a GC recognizing Hoechst 33258 analogue to the decadeoxyribonucleotide d-[CATGGCCATG]2: structural and dynamic aspects deduced from high field 1H-NMR studies. *J Biomol Struct Dyn* 1990;8:331–357.
54. Rao KE, Lown JW. Molecular recognition between ligands and nucleic acids: DNA binding characteristics of analogues of Hoechst 33258 designed to exhibit altered base and sequence recognition. *Chem Res Toxicol* 1991;4:661–669.
55. Singh MP, Joseph T, Kumar S, Bathini Y, Lown JW. Synthesis and sequence-specific DNA binding of a topoisomerase inhibitory analog of Hoechst 33258 designed for altered base and sequence recognition. *Chem Res Toxicol* 1992;5:597–607.